

DOI: 10.24850/j-tyca-14-01-08

Notes

Assessment of the potential recharge by infiltration in the northern zone of Loreto, Baja California Sur, Mexico

Estimación de la recarga potencial por infiltración en la zona norte de Loreto, Baja California Sur, México

Mario Verdugo¹, ORCID: <https://orcid.org/0000-0002-4070-1018>

Oscar Arizpe², ORCID: <https://orcid.org/0000-0002-2155-2678>

¹Universidad Autónoma de Baja California Sur, La Paz, Mexico,
mverdugo_15@alu.uabcs.mx

²Universidad Autónoma de Baja California Sur, La Paz, Mexico,
oarizpe@uabcs.mx

Corresponding author: Mario Daniel Verdugo,
mverdugo_15@alu.uabcs.mx

Abstract

This study assesses an estimate of the potential rainfall infiltration in the northern area of Loreto in the state of Baja California Sur, Mexico. The



2023, Instituto Mexicano de Tecnología
del Agua. Open Access bajo la licencia CC BY-NC-SA 4.0
(<https://creativecommons.org/licenses/by-nc-sa/4.0/>)

Tecnología y ciencias del agua, ISSN 2007-2422,
14(1), 333-390. DOI: 10.24850/j-tyca-14-01-08

basins of Gombedor, Loreto, and San Bruno are included. The analysis is based on precipitation and temperature data from the climatic stations near the municipality of Loreto. This study is in response to the scarcity within the matter and the urgency that the pressure on water resources represents to the region. Precipitation and temperature models were estimated using the Kriging interpolation method. The evapotranspiration, runoff, and potential infiltration were calculated from these models. The results obtained were 5.37 Mm³ year-1 for the Gombedor basin, 13.37 Mm³ year-1 in the San Bruno basin, and 7.62 Mm³ year-1 north of Loreto. The San Bruno basin is where the extraction wells that supply the city of Loreto are located. In the San Bruno basin, a potential recharge of 1.97 Mm³ year-1 was estimated with an average annual rainfall of 207 mm. Rainfall infiltration is one of the most important sources of aquifer recharge, in addition to groundwater flows and induced recharge. The hydrogeological model allows for addressing the situation of the basin to develop management strategies. These models can be efficient in regions without surface waters and readily available information. Moreover, hydrogeological models provide a good forecast for the Loreto region since the data are insufficient. The results for the variables show the potential of the methods based on techniques of Geographical Information Systems and geostatistics.

Keywords: Natural recharge, modeling of climatic variables, interpolation, Kriging, water balance, Loreto.



Resumen

En este estudio se realiza una estimación de la recarga potencial por infiltración de lluvia en la zona norte de Loreto en el estado de Baja California Sur, México, donde se incluyen las cuenca de Gombedor, Loreto y San Bruno; ello, en respuesta a la escasa información en el área y la urgencia que representa la presión sobre los recursos hídricos. A partir de datos de precipitación y temperatura de las estaciones climáticas cercanas al municipio de Loreto se realizaron modelos de precipitación y temperatura mediante el método de interpolación Kriging; con estos modelos se calcularon la evapotranspiración, el escurrimiento y finalmente la infiltración potencial. Los resultados obtenidos fueron de 5.37 Mm³ año-1 para la cuenca de Gombedor, 13.37 Mm³ año-1 en la cuenca de San Bruno y 7.62 Mm³ año-1 en el norte de Loreto. En la cuenca San Bruno se encuentran los pozos de extracción que surten a la ciudad de Loreto, aquí se estimó una recarga potencial de 1.97 Mm³ año-1 con una precipitación media anual de 207 mm. La infiltración por la lluvia es una de las fuentes más importantes de recarga de los acuíferos, junto con los flujos subterráneos, y la recarga artificial o inducida. El modelo hidrogeológico conceptual permite abordar más fácilmente la situación de la cuenca para elaborar estrategias de manejo. Este tipo de modelos puede resultar eficiente donde no hay aguas superficiales, ya que brinda un buen pronóstico para zonas con pocos datos o que son difícil acceso mediante el uso de técnicas de sistemas de información geográfica y geoestadísticas.



Palabras clave: recarga natural, modelado de variables climáticas, interpolación, Kriging, balance hídrico, Loreto.

Received: 13/01/2021

Accepted: 11/09/2021

Introduction

Water is an essential resource for life on earth. It is found in natural and human aspects. However, water is a resource of limited quantity in arid regions where the main source of supply is groundwater from aquifers. Water scarcity is the condition in which demand cannot be satisfied; the pressure from population needs has led to overexploitation in many aquifers worldwide (Water UN, 2012; WWAP, 2019). Overexploitation is an event that occurs in most of the aquifers in the state of Baja California Sur (BCS), and many of them are in critical condition (García-Gastelum *et al.*, 2013). As the main water source for human consumption, it is important to realize good aquifer management that can be achieved by quantifying groundwater and recharging. Groundwater recharge is when



rainwater infiltrates the soil into aquifers (Bureau of Reclamation & U.S. Department of the Interior, 1981). Other processes can contribute to aquifer recharge due to human activities, like agricultural irrigation, water distribution systems, dams, dikes, or stream banks (Ordoñez-Gálvez, 2011).

Different aquifer recharge assessment methods; are based on data from the saturated zone and others from the unsaturated zone and surface waters. The methods from the saturated zone generally provide more reliable estimates than those from unsaturated zones because they calculate the actual recharge; however, the data is not available in most cases and is costly to obtain. The methods from the unsaturated zone and surface waters estimate the potential recharge and result to be more imprecise. They are based on data such as precipitation, temperature, runoff, and evapotranspiration (Scanlon, Healy, & Cook, 2002). The hydrological balance can be calculated by equations or empirical relations already established in different basins and by modeling the variables that integrate it (Hakala, Addor, & Seibert, 2018; Macheckposhti, Sedghi, Telvari, & Babazadeh, 2018; Peña-Díaz, 2019; Martínez-Austria, Vargas Hidalgo, & Patiño-Gómez, 2019; Velázquez-Zapata & Troin, 2020). There are empirical estimations in basins from BCS (Cruz-Falcón *et al.*, 2013; Antonio, Martínez, Brandebourger, Mora, & Mahlknecht, 2017).

The quantification of natural recharge is a fundamental requirement to manage groundwater efficiently. Rainfall infiltration is one of the most important sources of aquifer recharge. Gomedor, San Juan Londó, and



Loreto aquifers are located North of Loreto. San Juan Londó aquifer is the largest source of potable water for Loreto Town, which has doubled its population in just 15 years, reaching more than 20,000 inhabitants today (Steinitz *et al.*, 2005; Gobierno de Baja California Sur, 2020). The population depends mainly on tourism. Here, the Natural Protected Area (NPA) Loreto Bay National Park is located, causing great pressure on the region from economic development (DOF, 1996). For several years it has been known that the San Juan Londó aquifer is in deficit; also, there is evidence that it presents saline intrusion (Wurl, Rodríguez, Cassassuce, Gutiérrez, & Velázquez, 2013). According to National Water Commission (Conagua in Spanish), the Loreto aquifer is also in deficit, but the extraction volume is lower than the San Juan Londó aquifer (Conagua, 2018a). In the present work, the potential recharge is estimated. Even though it is known that the estimations may be considered imprecise, the information available in this area is scarce and imprecise. The development of models to estimate hydrological variables is a great alternative when there is a lack of information or studies. This work aims to present a method to calculate the potential recharge by infiltration of rainwater in the northern area of Loreto BCS. The above was made by modeling the variables of precipitation, temperature, evapotranspiration, and runoff. Moreover, the estimation of the water balance was calculated with the residual method, which offers great flexibility in its application but has the limitation that the method relies on the accuracy with hydrological variables are calculated (Scanlon *et al.*, 2002).



Materials and methods

Study area

The study area is located in the central-eastern part of the Baja California peninsula in the Loreto municipality. It is located in the A. Frijol-A. San Bruno basin in the Hydrological Region HR06 BCS (La Paz). The study area has an extension of 1 299 km². The desert climate and the scarce rainfall cause the region's main runoff are intermittent, and no rivers with permanent flows. It presents runoff orientation from east to west. Therefore, the main discharge of the intermittent and ephemeral streams originated in the Sierra de la Giganta and flowed into the Gulf of California (INEGI, 2010). The study area includes San Bruno (647.5 km²), Gombedor (296.6 km²), and north of Loreto basins (355 km²) (Figure 1). The San Juan B. Londó valley is located in the San Bruno basin. In the valley is where potable water extraction is for Loreto Town and agricultural use (Conagua, 2018b). In front of these basins in the Gulf of



California, Loreto Bay has great biodiversity and commercial importance of many marine species, leading to the decree in 1996 as NPA (DOF, 1996). After the decree of the NPA, tourism became the most important economic activity for the region (Gobierno del Estado de Baja California Sur, 2020), which caused great pressure on water resources.



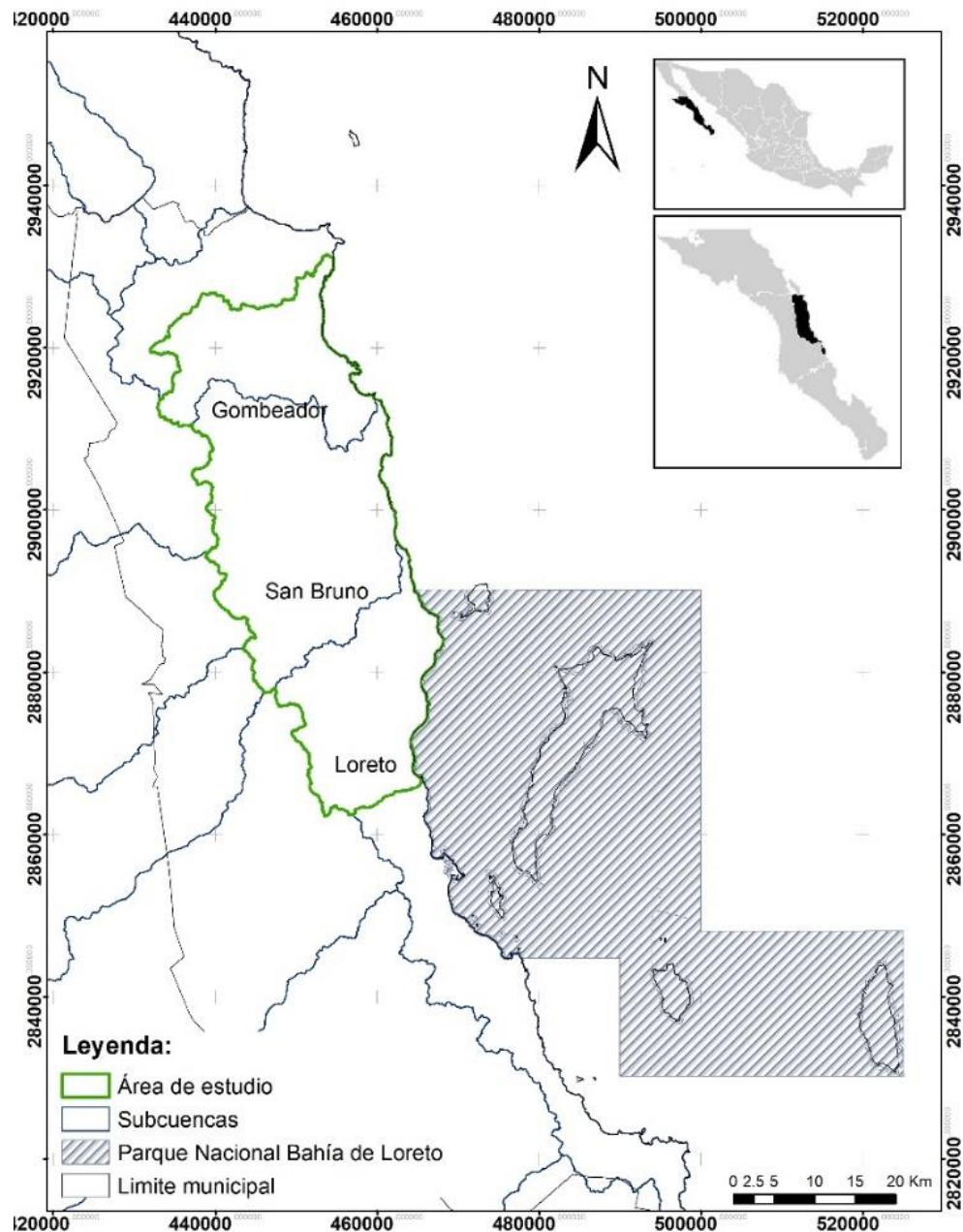


Figure 1. Map with the localization of the study area.

Data and analysis of the climatologic variables

The data were gathered from the climatic stations belonging to the Meteorological Monitoring Network of Conagua. The climatic stations are Comondú, La Poza Honda, La Purísima, Loreto, San Javier, San Juan Londó, San Ignacio de los Romero, Huatamote, La Poza de León, San Nicolás, San Antonio Norte, Liguí, San Lucas Norte y Guajademi (Table 1). Figure 2 shows the spatial distribution of the climatic stations. The daily climatology of the historical records of precipitation and temperature from the period 1986 to 2016 (Conagua, 2020) were averaged and added to obtain the total annual precipitation for each year. The exploratory data tests described below were carried out for the total annual precipitation.



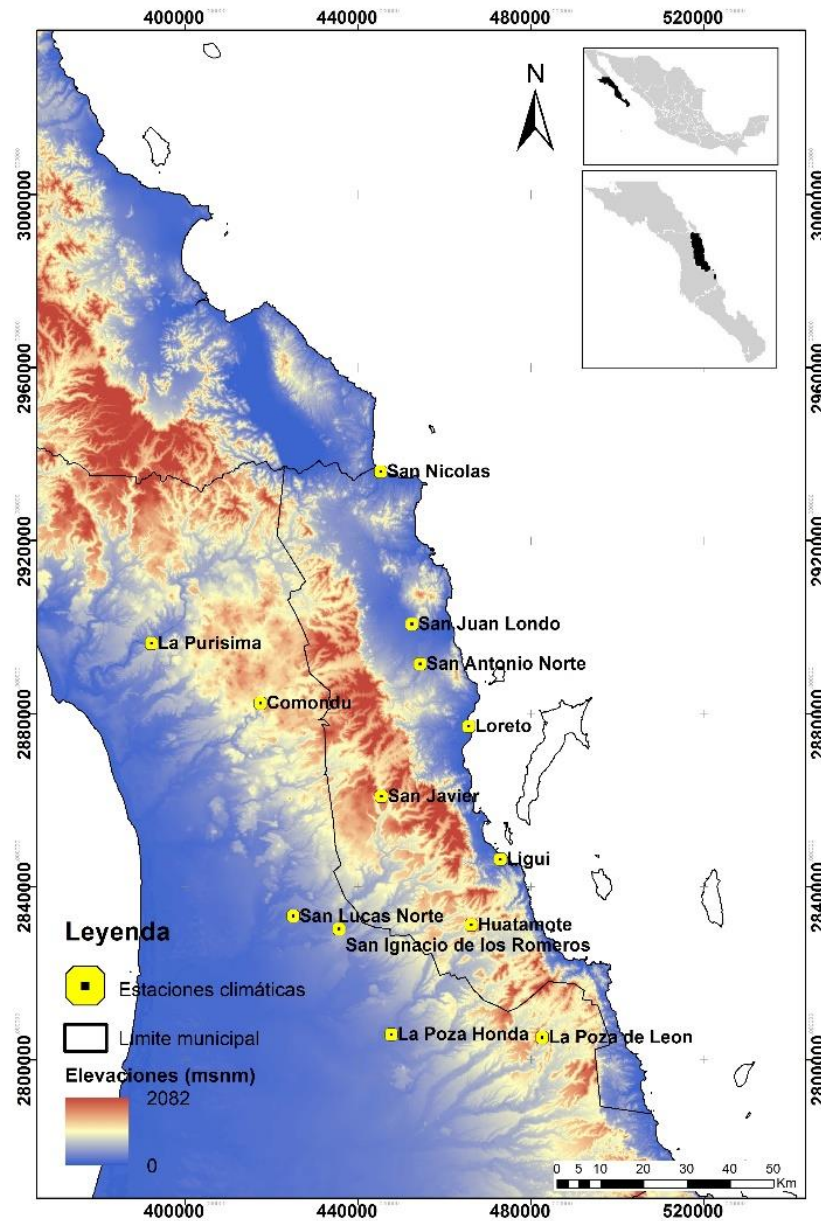


Figure 2. Spatial distribution of the climatic stations in the study area.



Table 1. Location of the climatic stations.

Station	Name	Coordinate X UTM	Coordinate Y UTM	Altitude (meters)
3008	Comondú	417475	2882401.2	300
3028	La Poza Honda	447744.3	2805809.4	20
3029	La Purísima	392299	2896275.4	95
3035	Loreto	465676.7	2877057.8	20
3054	San Javier	445455.2	2860879.9	200
3099	San Juan Londó	452553.7	2900688.5	40
3105	San Ignacio de los Romeros	435697.3	2830158.6	140
3108	Huatamote	466249.9	2831120.3	342
3109	La Poza de León	482674.7	2805099	360
3129	San Nicolás	445292.1	2935970.3	15
3133	San Antonio Norte	454419.3	2891489.5	100
3138	Liguí	472978.7	2846331.7	10
3141	San Lucas Norte	425088.3	2833137.7	200

Data consistency and homogeneity

An exploratory data analysis was performed for the recharge calculation of the basins (A. San Bruno, A. Gombedor y north of Loreto) since the information of the climatic stations may present some errors, such as the type of transcription or data printing error. Other errors may be poor instruments, observation errors, or missing data. Nevertheless, the missing data can be completed using mathematical methods. Table 2 shows the procedure for validating and estimating the missing data from climatological information according to Antonio *et al.* (2017) and Oliva, Gaytán, and González (2017).



Table 2. Statistical tests were performed to analyze and estimate missing data for the precipitation and temperature variables (period 1986-2016).

Data	Validation/consistency and homogeneity	Estimation of missing data
Precipitation	Atypical values	Pearson correlation
	Anderson Independence (Autocorrelación)	Z statistics
	Inconsistency (T-test)	Statistical efficiency
		Linear regression
Temperature	Atypical values	Normal
	Anderson Independency (Autocorrelación)	Normal ratio (3 stations)

The atypical value test was used to identify extreme data considered atypical in the precipitation series, and the software Minitab 17 was used (Minitab Inc., 2016). With the atypical value test, by not detecting atypical data, it can be considered that all the values of the sample come from a normally distributed population. The two samples' Student's t-test (T-



test) was also performed before and after filling in the data. This test allows us to verify the equality of the means of each sample. The series of precipitation data from each station were taken and divided into two blocks to compare the means of each block and obtain the $t > T$ statistic (T = distribution statistic) for each case; it was concluded whether each of the series is homogeneous. The T-test is powerful enough to detect inconsistency in the mean. It is also a robust test that is insensitive to the shape of the probability distribution of the series (Antonio *et al.*, 2017). Moreover, the Anderson independence test was performed with the autocorrelation serial, this test guaranteed that the series is composed of random variables. Autocorrelation is the mutual relationship between values of a time series in different periods, describing what happens to a value if there is a change in another value (Chereque, 1989). Autocorrelation measures the linear relationship between the observations of a data series Y_t and the distance from a time-lapse k ; the period k is known as lag. The lag denotes the period between the series values for which the type and degree of correlation of the variable considered are measured (Antonio *et al.*, 2017). Finally, a significance interval was constructed using the standard error using Minitab 17 software (Minitab Inc., 2016).



Missing data estimation method

The missing precipitation data for the annual averages for every station were calculated using the linear regression method (Oliva *et al.*, 2017). The linear regression method is based on the estimation of missing data for a station that is to be completed with another nearby station that contains more values, the correlation between the two stations was first established using Pearson's correlation. By having a relatively small sample, a test was performed to investigate whether this value can be equal to zero ($p = 0$) by estimating a Z statistic with the Equation (1) (Oliva *et al.*, 2017):

$$Z = \frac{\sqrt{n-3}}{2} \ln\left(\frac{1+r}{1-r}\right) \quad (1)$$

The Z statistic is calculated using the correlation coefficient r and the number of data n . Then the Z value obtained for each case was compared with $Z_c = 1.645$ and 95 % of confidence. If $Z \geq Z_c$, there is no possibility that p equals zero; therefore, the correlation coefficient is significant. Subsequently, the calculation of statistical efficiency (E) was carried out to know if the inference of the estimation of the values of X by the values of Y from the regression can be considered good (Equation (2)) (Oliva *et al.*, 2017):



$$E = 1 - r^2 \left(\frac{n-m}{n} \right) + \frac{n-m}{n(m-3)} (1 - r^2) \quad (2)$$

In Equation (2), the value of m corresponds to the total number of data from Y; n is the total number of data from X, and r is the correlation coefficient of X and Y. Where, if $E > 1$, it is not considered a good inference. If $E < 1$, it will be convenient to carry out the regression inference. Equation (3) was used to perform the linear regression.

$$y = b + mx \quad (3)$$

Where m is the slope of a line, and b is the ordinate to the origin. The method of the normal proportion of averages was used for the missing data of the temperature variable with three neighboring stations (Equation (4)) (Paulhus & Kohler, 1952):

$$P_x = \left[\left(\frac{N_x}{N_1} \right) P_1 + \left(\frac{N_x}{N_2} \right) P_2 + \left(\frac{N_x}{N_3} \right) P_3 \right] \quad (4)$$

Anderson's normality test was performed before applying the normal ratio formula (P_x). In Equation (4), N_x is the average of all the years from the temperature series of the station to be completed, N_1 , N_2 y N_3 is the average of the temperature series of each of the neighboring



stations used, and P_1 , P_2 , y P_3 is the average temperature of each neighboring season of the year to be completed.

Modeling of climatic variables

The Total Annual Precipitation (TAP) was obtained for each station by adding the monthly rainfall and then averaged for the 1986-2016 period; in the same way, the Average Annual Temperature (AAT) was obtained. Precipitation and temperature models were performed using a Geographic Information System (GIS) by interpolating the TAP and AAT data. Through the interpolation of the TAP, the precipitation model was made for the entire study area from the punctual data of the stations. The objective of interpolation is to estimate a function for an arbitrary point in a geographic space from the construction of a surface for that space that joins the points where the measurements have been made and whose value is known (Díaz-Padilla *et al.*, 2008). There are two groups of interpolation techniques: deterministic and geostatistical. The method used in this work was Kriging, which is among the geostatistical techniques. Kriging uses the sampling points' statistical properties that add to a statistical model that includes probabilities. It is important to mention that geostatistical methods provide an optimal prediction surface



and a measure of confidence about the probability. Kriging is also among the local methods as it only uses nearby sampling points when estimating (Emery, 2007; ESRI, 2009).

Furthermore, to avoid the edge effect, a greater number of stations that cover the total territory of the municipality of Loreto were used, and later a clip of the study area was made. Another point to mention about Kriging is that in the interpolation, it is possible to add another variable to the estimation of the main variable. Thus, the height in meters of the weather stations was used. Kriging uses the semivariograms, which quantify autocorrelation by plotting the variance of all pairs of data over a distance; to use the semivariogram, the assumptions of normality must be covered to prove that the data is stationary and must not have trends (Emery, 2007; ESRI, 2009). The software Sgems Beta v2.5b was used to obtain the semivariogram and the interpolation model. Afterward, the data from the semivariogram was entered in the Geostatistical Analyst extension of ArcGIS 10.2.2 and thus obtained the TAP and AAT interpolation maps.



Estimation of potential recharge by infiltration of rainfall

The real evapotranspiration model was calculated using the Turc empirical formula modified by Cruz-Falcón *et al.* (2011) for the region of BCS; the input data were from ATP and AAP models (Formula 5).

$$Et = \frac{P}{\sqrt{1.5 + \frac{P^2}{L}}} \quad (5)$$

In Equation (5), P is the precipitation in mm, $L = 300 + 25 T + 0.05 T^2$, where T is the temperature in °C.

To estimate the basin's recharge, the runoff model was calculated from obtaining the basin's runoff coefficient (Ce). The Ce represents how much precipitation effectively runs off the surface. The corresponding Equation (6) shows how the Ce was obtained (DOF, 2015):

$$Ce = K \frac{(P-250)}{2000} + \frac{(K-0.15)}{1.5} \quad \text{for } K > 0.15 \text{ and } Ce = K \frac{(P-250)}{2000} \quad \text{for } K < 0.15 \quad (6)$$

Equation (6) uses a parameter K that depends on the use and type of soil and precipitation. The information from the INEGI maps of soil



(series II) and soil use and vegetation (series VI) was used to obtain the parameter K (Figure 3 and Table 3). Some K values are in NOM-011-can-2000 (DOF, 2015); for vegetation that is not in the NOM, K values were assigned according to its similarity with other vegetation (Cruz-Falcón *et al.*, 2011). The K parameter is dimensionless and was obtained by classifying the basin soils as highly permeable, moderately permeable, and slightly permeable, according to the soil texture for each category of land use and vegetation. The values of parameter K are in Table 4.



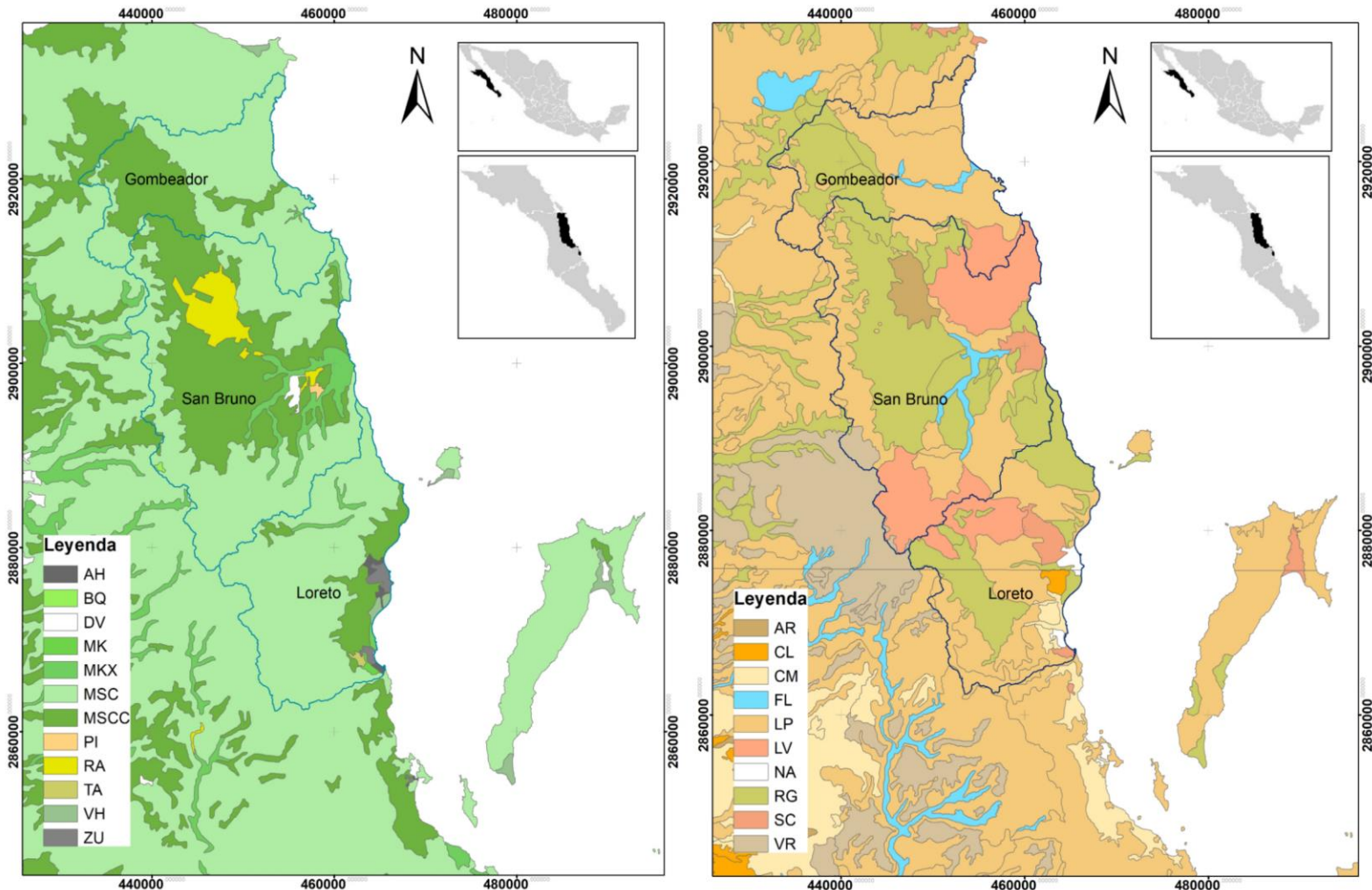


Figure 3. Maps of land use and vegetation (left) and soil map (right) showing the dominant soil of the study area (legend for maps is presented in Table 3).

Table 3. Inscription of the land use and edaphology study area showing the dominant soil.

Land use and vegetation	Meaning	Primary soil	Meaning
AH	Human settlements	AR	Arenosol
BQ	Oak forest	CL	Calcisol
DV	No apparent vegetation	CM	Cambisol
MK	Mesquite forest	FL	Fluvisol
MKY	Xerophile mezquital	Lv	LUvisol
MSC	Sarcocaule scrub	NA	No disponible
MSCC	Sarco-crasicaule scrub	RG	Regosol
PI	Induced grassland	SC	Solonchak
RA	Annual irrigation agriculture	VR	Vertisol
TA	Annual rainfed agriculture		
VH	Halophytic vegetation		
ZU	Urban zone		



Table 4. Parameter K values for vegetation according to land use in the study area.

Land use and vegetation	Very permeable	Moderately permeable	Less permeable
Agricultural area	0.24	0.27	0.30
Forest (oak 25-50% cover)	0.17	0.26	0.28
Induced grassland (50%)	0.24	0.28	0.30
Scrub (sarcocaule, sarco-cracicaule)	0.16	0.23	0.28
Mesquital	0.12	0.22	0.26
No apparent vegetation	0.26	0.28	0.30
Buildings	0.28	0.29	0.32

Applying Equation (6), the Ce was obtained for each basin. Then, with the product of Ce and the precipitation model, the runoff model was obtained. Finally, the infiltration model was calculated, where the precipitation, evapotranspiration, and runoff models were subtracted according to Equation (7), and the units of the variables were in mm.



From the digital models obtained, the annual recharge volume for the study area was calculated:

$$I = P - Et - Es \quad (7)$$

Where I = infiltration, P = precipitation, Et = evapotranspiration, and Es = runoff.

Results

Following what is described in the materials and methods section forthcoming, the results for the analysis of climatic variables, creation of models, and the estimation of recharge for the basin are described.



Data consistency and homogeneity

The results for the atypical data test showed atypical values in the 3008-Comondu and 3099-San Juan Londó stations, so those values were eliminated for subsequent calculations. The precipitation data for station 3099-San Juan Londó turned out to be inconsistent. This, in most cases, is enough evidence to rule out the station. However, it was decided to keep the station series because it is located in the most important aquifer for the region, and the data is considered relevant. For station 3099-San Juan Londó, another statistical test of normality and equality of variances was carried out with satisfactory results ($P = 0.11$). The normality test for temperature data in stations 3109-La Poza de León and 3138-Lugüi was not satisfactory, for which in both cases, Student's t and Helmert tests were performed for data consistency, with satisfactory results for station 3138-Ligüi. It was decided to discard station 3109-La Poza de León for presenting inconsistent data. The results of the statistical tests for precipitation and temperature are shown in Table 5 and Table 6.

Table 5. Result of the statistical tests of the precipitation series.

Station	Name	Anderson	T-Student



3008	Comondú	Independent	Homogeneous
3028	La Poza Honda	Independent	Homogeneous
3029	La Purísima	Independent	Homogeneous
3035	Loreto	Independent	Homogeneous
3054	San Javier	Independent	Homogeneous
3099	San Juan Londó	Independent	Not Homogeneous
3105	San Ignacio de los Romeros	Independent	Homogeneous
3108	Huatamote	Independent	Homogeneous
3109	La Poza de León	Independent	Homogeneous
3129	San Nicolás	Independent	Homogeneous
3133	San Antonio Norte	Independent	Homogeneous
3138	Liguí	Independent	Homogeneous

3141	San Lucas Norte	Independent	Homogeneous
-------------	-----------------	-------------	-------------

Table 6. Result of the exploratory analysis of the temperature series.

Station	Name	Normal	Anderson
3008	Comondú	Yes	Independent
3028	La Poza Honda	Yes	Independent
3029	La Purísima	Yes	Independent
3035	Loreto	Yes	Independent
3054	San Javier	Yes	Independent
3099	San Juan Londó	Yes	Independent
3105	San Ignacio de los Romeros	Yes	Independent
3108	Huatamote	Yes	Independent
3109	La Poza de León	No	Independent



3129	San Nicolás	Yes	Independent
3133	San Antonio Norte	Yes	Independent
3138	Liguí	No	Independent
3141	San Lucas Norte	Yes	Independent

Estimation of missing data

The correlation test (R) was carried out between two stations, showing the results in Table 7. In all cases, it was obtained a correlation greater than 0.8. The Z statistic is shown in Table 8, and it is inferred that the correlation's R can be considered significant.



Table 7. Results for the regression of missing precipitation data.

Station (X)	Station (Y)	R ²
Loreto	San Nicolás	0.59
Loreto	San Juan Londó	0.75
San Juan Londó	San Antonio Norte	0.69
San Juan Londó	Loreto	0.66
Huatamote	San Javier	0.78
La Poza de León	Huatamote	0.68
San Javier	Comondú	0.56
San Ignacio de los Romero	San Lucas Norte	0.73
San Ignacio de los Romero	La Poza Onda	0.66



Table 8. Results of the correlation tests between stations for the estimation of missing precipitation data.

Station (X)	Station (Y)	R	K	$\geq Zc$	E
Loreto	San Nicolás	0.7 7	3 0	5.30 1	0
Loreto	San Juan Londó	0.8 6	2 9	6.59 4	0.00 9
Loreto	San Antonio Norte	0.7 7	2 4	4.78 5	0.08 4
Ligui	Loreto	0.8 1	3 0	5.85 6	0.11 8
Huatamote	San Javier	0.8 8	2 8	7.01 5	0.00 8
La Poza de León	Huatamote	0.8 2	3 0	6.01 0	0.01 1
San Javier	Comondú	0.8	2 7	5.49 3	0.01 6
San Ignacio de los Romero	San Lucas Norte	0.8 5	2 8	6.28 0	0.03 0
San Ignacio de los Romero	La Poza Onda	0.8 1	2 7	5.52 1	0.05 2



Through linear regression, it was possible to estimate the data for a station X with missing data for Y. The results of the linear regression are shown in Table 8. Figure 4 shows an example of the linear regression result to complete the stations' data.

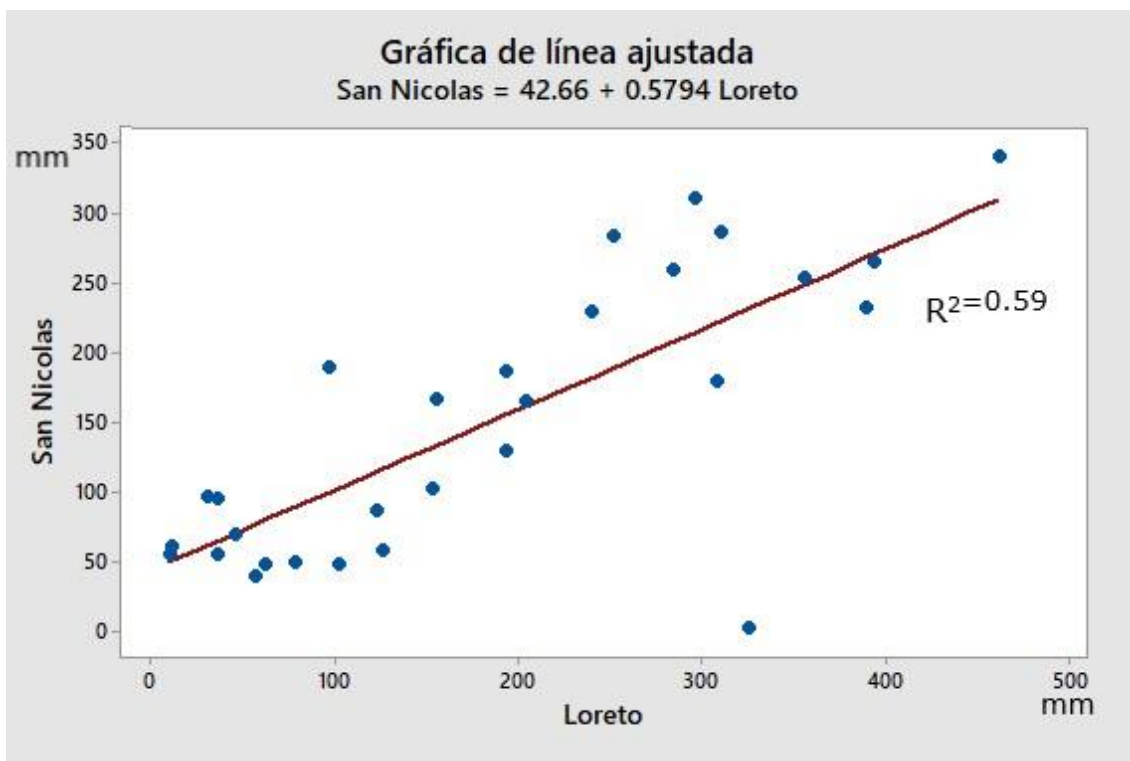


Figure 4. E. g. of the linear regression for TAP (mm) used to estimate the missing data from the San Nicolás station with the Loreto station.



Modeling of climatic variables

The TAP and AAT were obtained for each station by adding the monthly rainfall, and then the results were averaged for 1986. The results for TAP and AAT are showed in Table 9.

Table 9. TAP and AAT were used to interpolate the precipitation and temperature models.

Station	Name	TAP	AAT
3008	Comondú	204.9	22.9
3028	La Poza Honda	228.6	24.6
3029	La Purísima	137.5	22.9
3035	Loreto	184.3	24.7
3054	San Javier	232.1	22.1
3099	San Juan Londó	204.4	23.5
3105	San Ignacio de los Romeros	184.6	22.8
3108	Huatamote	277.5	22.9
3109	La Poza de León	247.5	22.6
3129	San Nicolás	148.2	23.7



3133	San Antonio Norte	238.6	23.5
3138	Liguí	235.9	23.6
3141	San Lucas Norte	232.4	21.4

As mentioned before, the data was subjected to statistical tests and thus was able to meet the assumptions required by the Kriging interpolation method. For TAP, the normality was verified through the Anderson-Darling test: mean = 212, standard deviation = 39.9, and $P = 0.311$. In the same way, the normality for AAT was verified: mean = 22.85, standard deviation = 0.97, and $P = 0.35$. The precipitation model presented a trend, which was removed with a first-order function of the linear Kernel function. With 30.04 goodness of fit, a measure that depends on the magnitude of the data turned out to be the best fit.

Furthermore, anisotropy was detected in the data, meaning that the correlation of the samples is dependent on the direction. Anisotropy is detected by studying the data set in different directions, indicating that the regionalization is more intensely structured in some directions than others. The anisotropy was found at 337° . The size of the lag was determined using the nearest neighbor average method that resulted from 20,748.32 meters. Similarly, the temperature model presented a very marked upward trend from east to west and a trend that decreased in a north-south direction. The effect of the first-order trend was removed with the linear kernel function, obtaining 1.04 goodness of fit. The size of the lag was determined using the nearest neighbor average method that



resulted from 19,349.87 meters. Finally, the Kriging interpolation was carried out using the height of the stations as the second variable, and the Geostatistical extension Analyst of ArcGIS 10.2.2 was used. The models obtained for precipitation and temperature of the study area are shown in Figure 5.

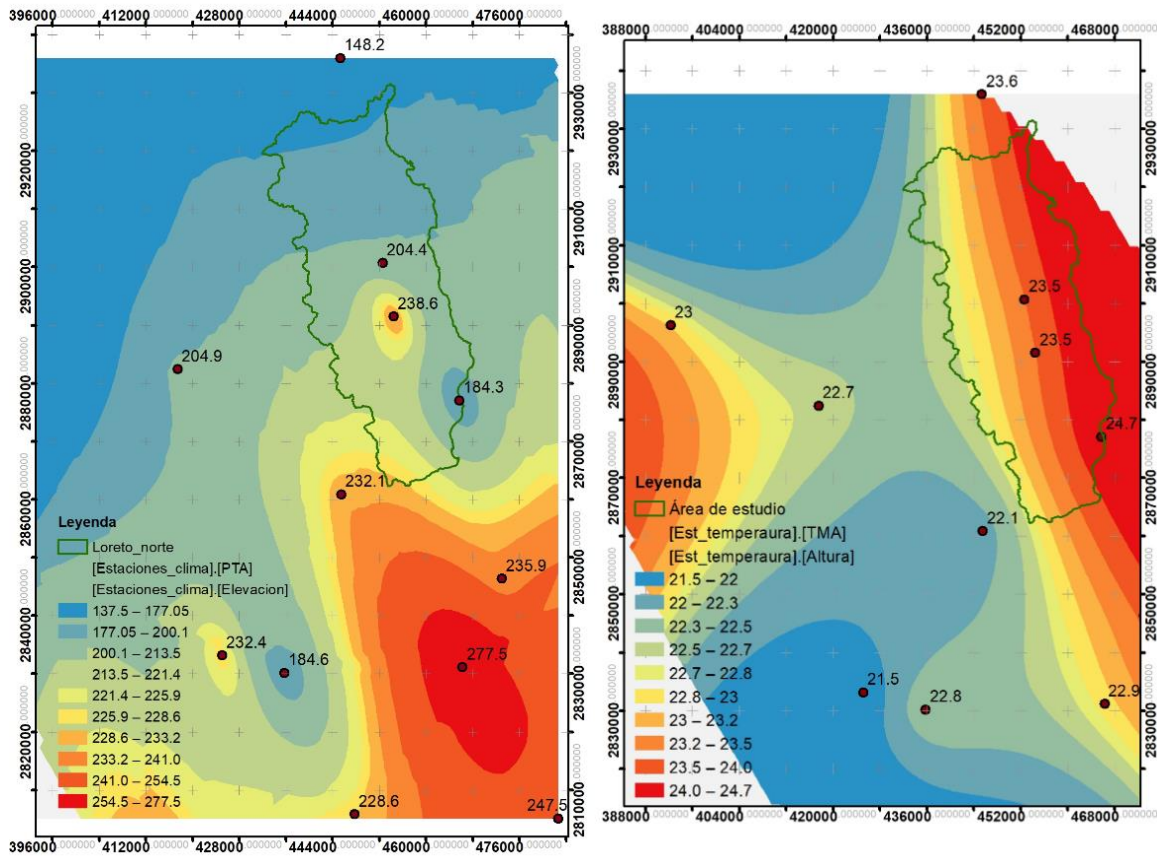


Figure 5. The precipitation model (left) and temperature model (right) of the study area are made by Kriging interpolation.



The measurements of the error for the models are found in Table 10. In the prediction of the precipitation model, a mean square error (MSE) of 33.04 mm was found. The standardized MSE was 1.27, which quantifies the reliability of the standard errors of the prediction. The prediction is considered accurate if the standardized MSE is close to one. Regarding the temperature model, the average of the errors indicates that in the mean predictions, the temperature is -0.17 °C distant. MSE for the temperature model was 0.80 °C, and the average error is standardized (-0.62). It is required to validate the standardized error, and in addition to making predictions, the variability of these concerning the real values is estimated. If the standard error is close to the MSE, the assessment of the variability in the estimate is considered correct. Since the standard error is less than the mean square error, the prediction's variability is underestimated. The standardized mean square error should be close to one (ESRI, 2009).

Table 10. Error measurements for the prediction of values in the models.

	Precipitation	Temperature
Mean error	4.40	-0.17
Mean square error	33.04	0.80
Mean error standardized	0.12	-0.64
Standardized mean square error	1.27	2.96



The geostatistical layers of precipitation and temperature were converted into a raster format. For the conversion, the software uses block interpolation. The block interpolation method predicts the average value of a specific area, which corresponds to the desired cell size in the raster. This step is important since it will affect the subsequent calculations of the model. During the conversion, the number of prediction points used in the X and Y direction is specified to obtain the mean of each cell. The prediction made for each number of points identifies the original geostatistical layer and the original sampling points (climatic stations). The number of points selected will depend on the location of the points, trying to capture the directional trend. The bibliography recommends a more significant number of points in the direction where there are more samples to capture the more significant variability of the greater number of samples (Chiles & Delfiner, 1999; ESRI, 2009). The raster maps of precipitation and temperature with a resolution of 100x100 meters are shown in Figure 6.



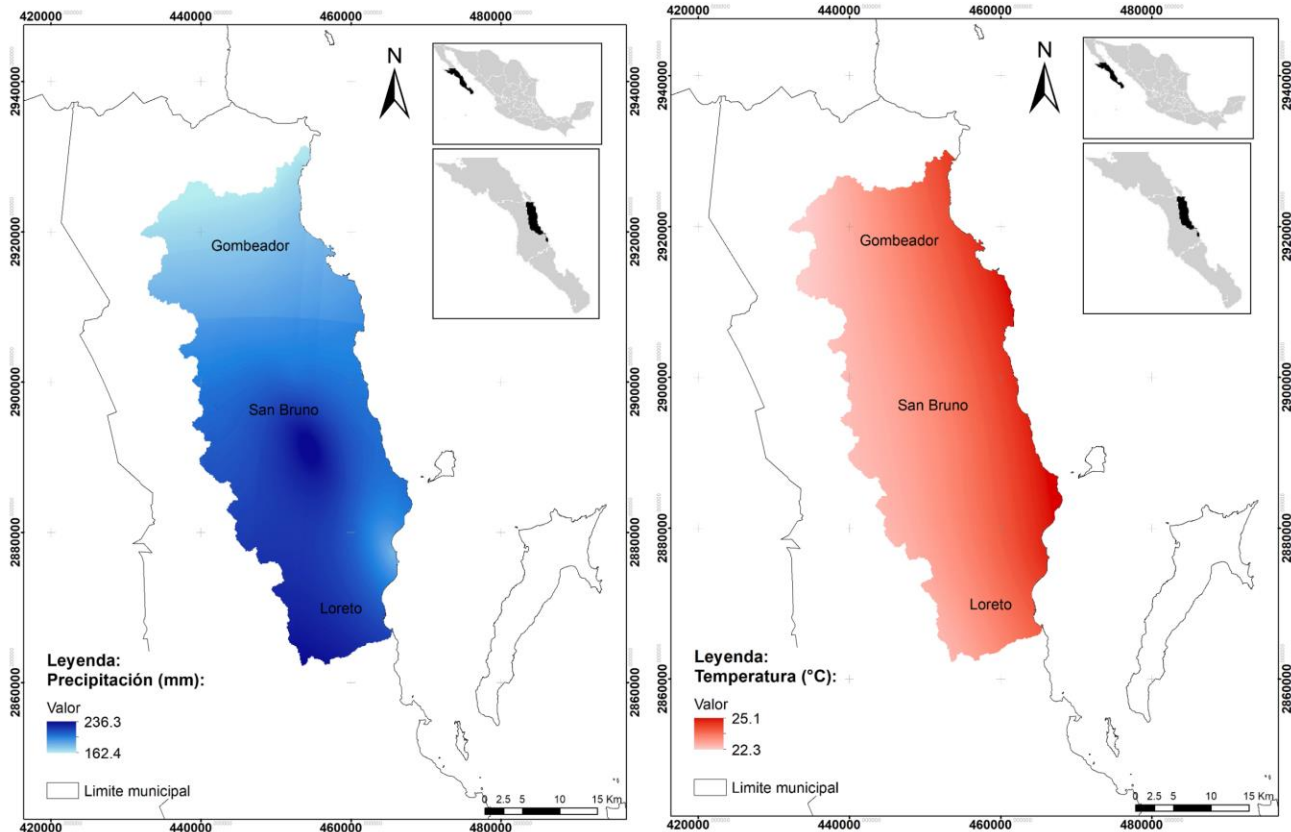


Figure 6. Raster maps of precipitation (mm) and temperature (°C).

The precipitation model shows higher values in the central and southern parts of the study area, especially in the San Bruno basin. The mean precipitation was 181.7 mm ($sd = 6.1$) for the Gombedor basin (north of the study area), with minimum values of 164.3 mm and maximums of 198.4 mm. For Loreto north basin, a mean of 214.3 mm ($sd = 8.8$) was estimated, with minimum values of 186.4 mm and maximums de 231.1 mm. Finally, for the San Bruno basin, the mean

precipitation was 207 mm ($sd = 11.1$), with minimum values of 182.3 mm and maximums of 236.3 mm. The temperature model shows a gradient in the study area from 22.3 to 25.1 °C, where the maximum average annual temperatures occur in the coastal region of the Gulf of California. The minimum temperatures occur in the highest region of the Sierra de la Giganta east of the study region. Generally, there is a difference of 3 °C across the area.

Estimation of potential recharge by infiltration

The evapotranspiration was calculated with the result obtained in the precipitation and temperature models. The evapotranspiration model was calculated following the materials and methods section; the result is shown in Figure 7.



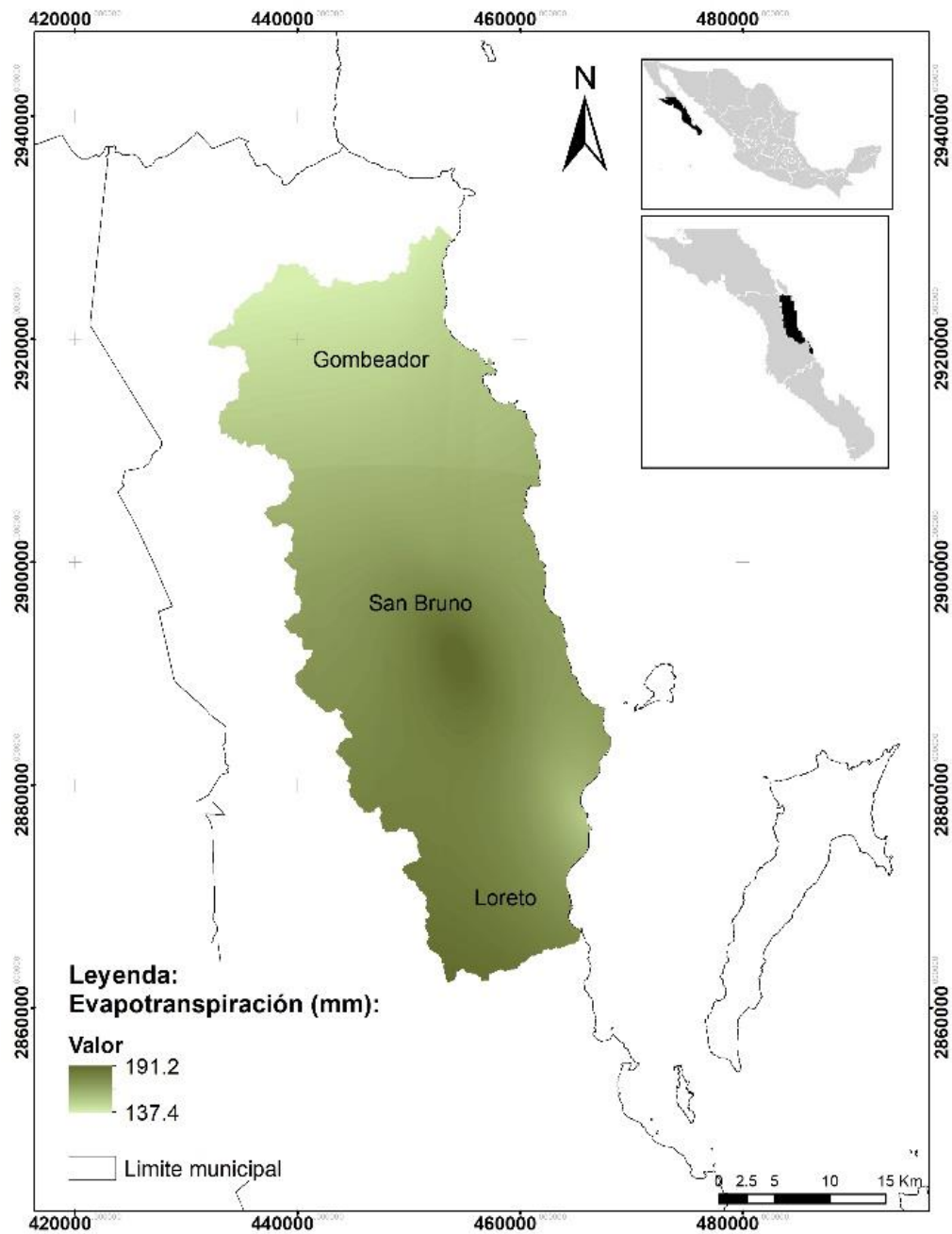


Figure 7. Evapotranspiration (mm) for the study area.

Afterward, the runoff model was estimated by obtaining the runoff coefficient (C_e), and then using the precipitation model, calculated the potential runoff for each basin (Figure 8).

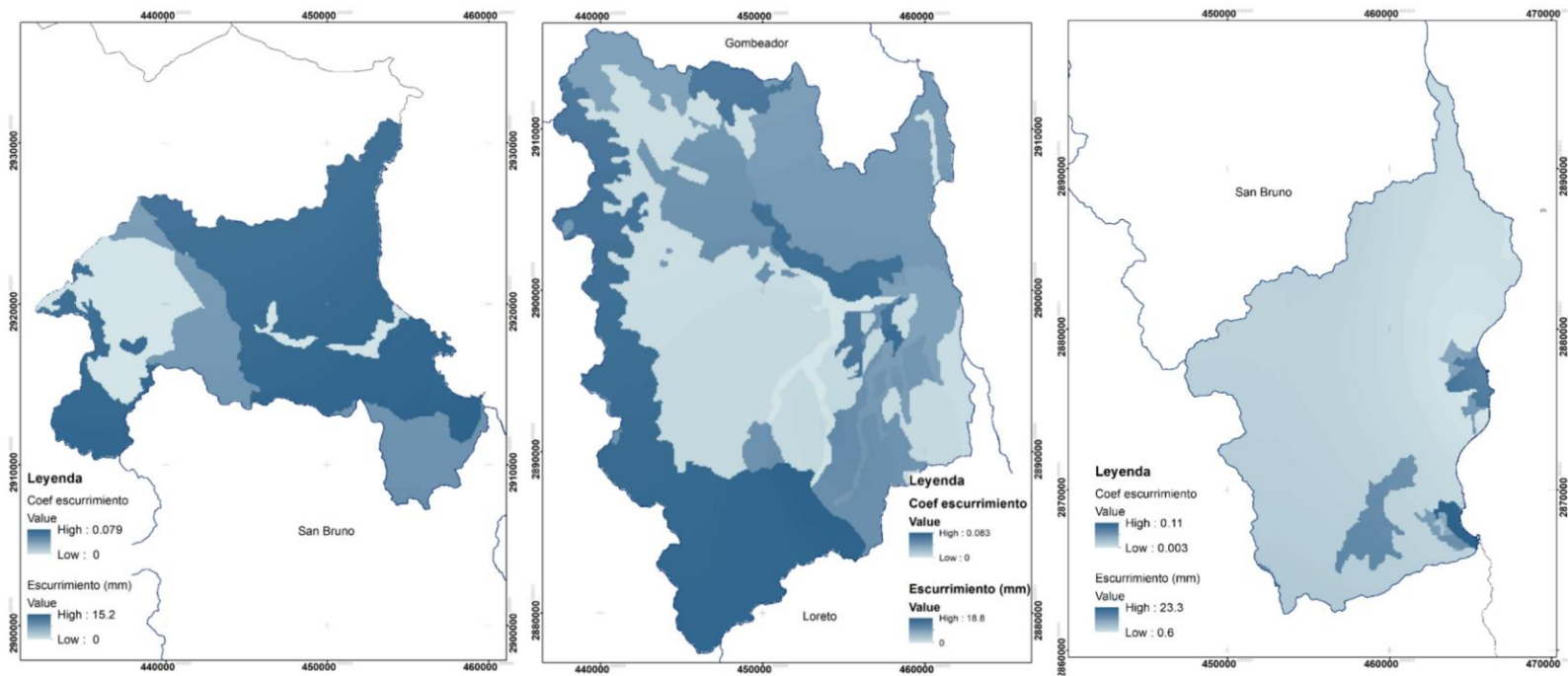


Figure 8. Runoff models (mm) for each basin, Gombedor (left), San Bruno (center), and North of Loreto (right).

Finally, the infiltration model was calculated (Figure 9). The evapotranspiration and runoff models were subtracted from the precipitation model. It was possible to estimate the potential recharge of



each one of them through the water balance. The water balance for recharge by infiltration of rainwater for the basins is found in Table 11.

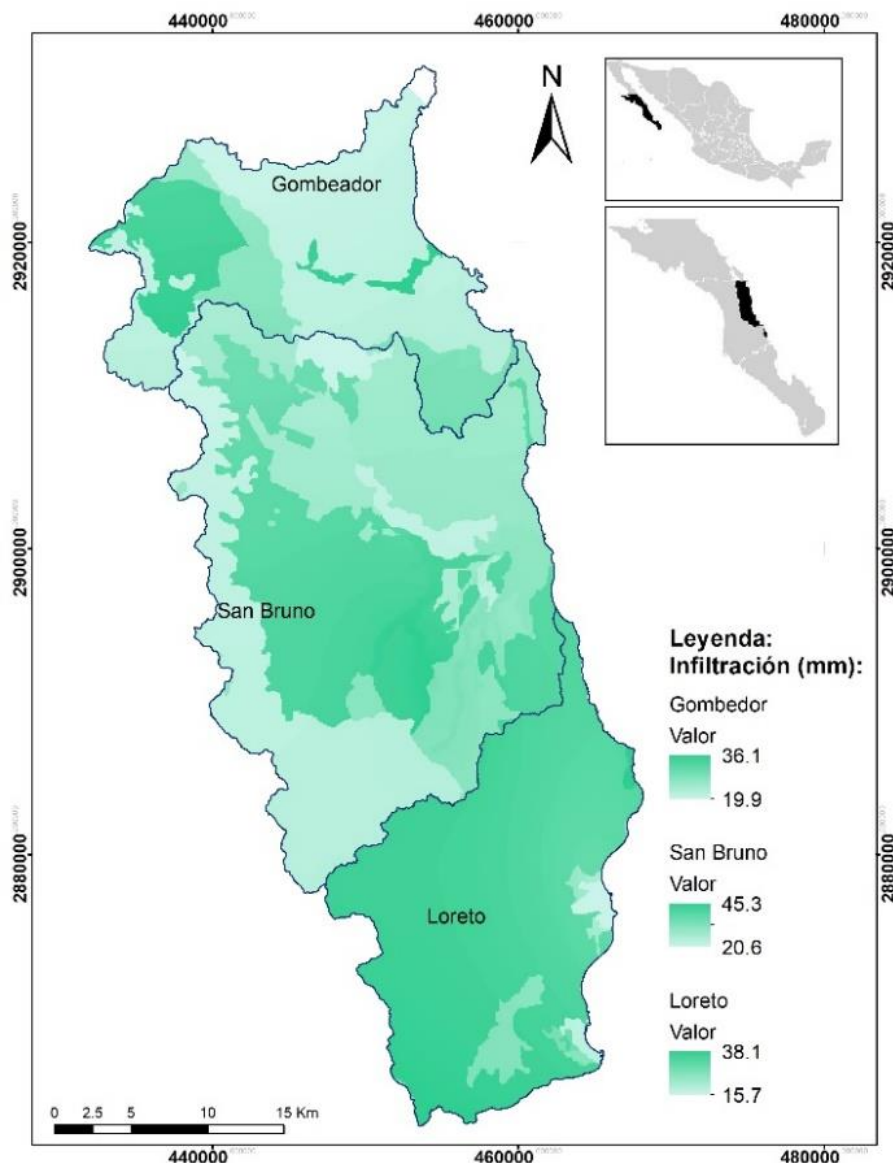


Figure 9. Infiltration (mm) for each basin in the study area.



Table 11. Water balance in each of the basins in the study area.

	Gomedor (Mm³ year⁻¹)	%	San Bruno (Mm³ year⁻¹)	%	Loreto (Mm³ year⁻¹)	%
Precipitation	5.37	100	13.37	100	7.62	100
Evapotranspiration	4.30	80.1	10.84	81.1	6.18	81.1
Runoff	0.31	5.8	0.56	4.2	0.39	5.1
Infiltration	0.73	13.6	1.97	14.7	1.05	13.8

Discussion

The precipitation model shows higher values to the south of the study area in the Sierra de la Giganta at about 1200 meters above mean sea level (mamsl) and in the central part of the San Bruno basin. In the Loreto basin, an average annual rainfall of 214.3 mm ($sd = 8.8$), minimum values of 186.4 mm, and a maximum of 231.1 mm; for this area, the average annual record is 190 mm (Conanp, 2002; Conagua, 2018a). The mean annual precipitation for the San Bruno basin was estimated at 207



mm ($sd = 11.1$), a minimum of 182.3 mm, and a maximum of 236.3 mm. The climatic stations of San Juan Londó and San Antonio Norte are located within this basin; according to Conagua (2018b), the annual average is 143 mm, with a maximum of 387 mm associated with cyclonic events. For the Gomedor basin north of the study area, an annual mean of 181.7 mm ($sd = 6.1$), minimum of 164.3 mm, and maximum of 198.4 mm.

It should be noted that in this basin, there is no climatic station, so there are no data available for the average precipitation or any estimate, which shows the importance of the model for the area as a first approximation. Additionally, the Gomedor basin is under pressure from tourism, and conservation efforts have recently been carried out (Vanderplank, Favoretto, Mascareñas, & Aburto, 2020). Generally, average annual precipitation of 200 mm is calculated for BCS and varies from 150 to 300 mm across the state (Antonio *et al.*, 2017; Conagua, 2018a).

The highest evapotranspiration values occur when there is an incidence of higher precipitation in the center and southeast of the study area, which is feasible. Turc's method for calculating real evapotranspiration is one of the most widely used. The method is based on observations made in many basins with different climates distributed worldwide and is recognized to give very good results (Sánchez-Martínez & Carvacho-Bart, 2011). Evapotranspiration represented over 80% in the three basins with values ranging from 137 to 191 mm, and a similar result

was found in other basins using Turc's method for real evapotranspiration (Cruz-Falcón *et al.*, 2011; Peña-Díaz, 2019).

In the San Bruno basin, the infiltration model estimated a potential annual infiltration of 1.97 Mm³. The study carried out by the former Secretariat of Hydraulic Resources (SARH) in 1978 estimated an annual infiltration of 1.8 Mm³ (Conagua, 2018b). At the same time, Steinitz *et al.* (2005) estimated an annual infiltration of 2 Mm³ with a low average annual precipitation and storm every two years. Subsequently, the official decree of availability of the aquifer estimated an annual infiltration of 1.3 Mm³ with an average yearly rainfall of 200 mm (207 mm in this paper). In the San Bruno basin, the wells supply Loreto Town. According to official data, the concessions are 3.561 Mm³ annually for potable use and 2.76 Mm³ annually for agricultural use (Conagua, 2018b). It is recognized that the aquifer has been overexploited for several years (Lesser, Meza, Castañon, & González, 2006; Wurl *et al.*, 2013).

Rainwater infiltration is influenced by various factors such as vegetation cover, topography, type of soil, and physical factors such as porosity and hydraulic conductivity. The method to estimate the potential recharge by infiltration is from the surface variables, where the rainfall may or may not reach the water table due to processes of the unsaturated zone, constituting the diffuse recharge of groundwater (Scanlon *et al.*, 2002; Zhao, Jiang, Wang, & Wan, 2021). Water movement is predominantly vertical in areas with diffuse recharge potential, and the San Juan Londó aquifer is shallow with granular sedimentary material,



which can benefit vertical recharge (González-Abraham, Fagundo-Castillo, Carrillo-Rivera, & Rodríguez-Estrella, 2012; Zhao *et al.*, 2021). As part of the infiltration calculation, the runoff coefficient was used, which is dependent on the use of soil, vegetation, and the type of dominant soil, taking into account the permeability of this. The water balance was calculated using the residual method, considered an indirect method (Scanlon *et al.*, 2002). The limitation of the residual method is that the estimate depends on the accuracy and reliability of the components used for the calculation (precipitation, evapotranspiration, runoff). Moreover, an advantage of applying spatial models is that it allows identifying recharge areas vulnerable to aquifer contamination.

Conclusions

This study presented a methodology to estimate the potential recharge by infiltration in a basin from precipitation and temperature data. In Mexico, there is the Meteorological Monitoring Network of Conagua. However, these often present incomplete data, so an estimate was made to complete them through effective methods. Interpolation models require as many points as possible, being a powerful tool for predictions;



if used best, the geostatistical method returns a measure of error in the prediction.

Modeling the hydrological variables makes it possible to address the identification of the recharge sites, transit and discharge zones of groundwater to establish management actions on the aquifer through the protection and sustainable use of groundwater. Furthermore, this study allowed us to identify areas where it is shown that there is a hydrological connection between the surface water and the aquifer through the infiltration model. The potential for improvement is incorporating remote sensing tools to verify the models. However, the types of methods presented in this work are efficient with no surface water for use since they provide a good forecast for areas with little data or difficult to access.

Acknowledgment

This study was carried out with the support of a Conacyt scholarship at the Coastal Systems Ecology Laboratory of the Autonomous University of Baja California Sur.



References

- Antonio, A. H., Martínez, M. J. A. T., Brandebourger, M. N. I., Mora, A., & Mahlknecht, J. (2017). *Modelación numérica para la determinación de flujos subterráneos. Sitio piloto: La Paz, Baja California Sur, México*. Monterrey, México: Centro del Agua para América Latina y el Caribe., Nuevo León, México.
- Bureau of Reclamation & U.S. Department of the Interior. (1981). *Ground water manual: A water resources technical publication. A guide for the investigation, development, and management of groundwater resources*. Denver, USA: U.S. Department of the Interior, Water and Power Resources Services, Bureau of Reclamation.
- Chereque, W. (1989). *Hidrología para estudiantes de ingeniería civil*. Lima, Perú: Pontificia universidad Católica de Perú.
- Chiles, J. P., & Delfiner, P. (1999). *Geostatistics. Modelling spatial uncertainty*. New York, USA: John Wiley & Sons.
- Conagua, Comisión Nacional del Agua. (2018a). *Actualización de la disponibilidad media anual del agua en el acuífero Loreto (0328), Estado de Baja California Sur*. Ciudad de México, México: Diario Oficial de la Federación.
- Conagua, Comisión Nacional del Agua. (2018b). *Actualización de la disponibilidad media anual del agua en el acuífero San Juan Londó (0329), Estado de Baja California Sur*. Ciudad de México, México: Diario Oficial de la Federación.



Conagua, Comisión Nacional del Agua. (2020). *CNA-SMN-CG-GMC-SMAA-CLIMATOLOGIA. Base de datos climatológica a marzo de 2020.*

Recovered from

<https://smn.conagua.gob.mx/es/climatologia/informacion-climatologica/informacion-estadistica-climatologica>

Conanp, Comisión Nacional de Áreas Naturales Protegidas. (2002). *Programa de Manejo del Parque Nacional Bahía de Loreto.* México, DF, México: Dirección General de Manejo para la Conservación, Comisión Nacional de Áreas Naturales Protegidas.

Cruz-Falcón, A., Vázquez-González, R., Ramírez-Hernández, J., Navasánchez, E. H., Troyo-Diéguex, E., Rivera-Rosas, J., & Vega-Mayagoitia, J. E. (2011). Precipitación y recarga en la cuenca de La Paz, BCS, México. *Universidad y Ciencia*, 27(3), 251-263.

Cruz-Falcón, A., Ramírez-Hernández, J., Vázquez-González, R., Navasánchez, E. H., Troyo-Diéguex, E., & Fraga-Palomino, H. C. (2013). Estimación de la recarga y balance hidrológico del acuífero de la Paz, BCS, México. *Universidad y Ciencia*, 29(1), 87-100.

Díaz-Padilla, G., Sánchez-Cohen, I., Quiroz, R., Garatuza-Payán, J., Watts-Thorp, C., & Cruz-Medina, I. R. (2008). Interpolación espacial de la precipitación pluvial en la zona de barlovento y sotavento del Golfo de México. *Agricultura Técnica en México*, 34(3), 279-287.

DOF, Diario Oficial de la Federación. (19 de julio de 1996). *Decreto del Parque Marino Nacional Bahía de Loreto.* México, DF, México: Diario Oficial de la Federación.



DOF, Diario Oficial de la Federación. (2015). *Conservación del recurso agua-Que establece las especificaciones y el método para determinar la disponibilidad media anual de las aguas nacionales. NORMA Oficial Mexicana NOM-011-CONAGUA-2015.* México, DF, México: Diario Oficial de la Federación.

Emery, X. (2007). *Apunte de geoestadística.* Santiago, Chile: Facultad de Ciencias Físicas y Matemáticas, Universidad de Chile.

ESRI, Environmental Systems Research Institute. (2009). *ArcGIS Desktop Help.* ESRI Web Help. Recovered from <http://webhelp.esri.com/arcgisdesktop/9.3/index.cfm?TopicName=welcome>

García-Gastelum, A., Arizpe, O., Fermán-Almada, J. L., González-Baheza, A., Poncela-Rodríguez, L., Wurl, J., & Amador-Amao, M. (2013). *Programa de medidas preventivas y de mitigación de la sequía (PMPMS).* La Paz, México: Consejo de Cuenca Baja California Sur.

Gobierno de Baja California Sur. (2020). *Loreto, información estratégica.* La Paz, México: Dirección de Informática y Estadística, Secretaría de Turismo, Economía y Sustentabilidad.

González-Abraham, A., Fagundo-Castillo, J. R., Carrillo-Rivera, J. J., & Rodríguez-Estrella, R. (2012). Geoquímica de los sistemas de flujo de agua subterránea en rocas sedimentarias y rocas volcánicas de Loreto, BCS, México. *Boletín de la Sociedad Geológica Mexicana,* 64(3), 319-333.



Hakala, K., Addor, N., & Seibert, J. (2018). Hydrological modeling to evaluate climate model simulations and their bias correction. *Journal of Hydrometeorology*, 19(8), 1321-1337.

INEGI, Instituto Nacional de Estadística y Geografía. (2010). *Documento técnico descriptivo de la red hidrográfica escala 1:50 000*. Aguascalientes, México: Dirección General de Geografía y Medio Ambiente, Instituto Nacional de Estadística y Geografía.

Lesser, J. M., Meza, J. L., Castañon, V. M., & González, D. (2006). Funcionamiento del acuífero de San Juan Londó, B.C.S. y su relación con la intrusión con agua de mar. *Memorias 6º Congreso de Aguas Subterráneas, Asociación Geohidrológica Mexicana*, octubre 2007. Puerto Vallarta, Jalisco, México.

Machekposhti, K. H., Sedghi, H., Telvari, A., & Babazadeh, H. (2018). Modeling climate variables of rivers basin using time series analysis (case study: Karkheh River basin at Iran). *Civil Engineering Journal*, 4, 78.

Martínez-Austria, P. F., Vargas Hidalgo, A., & Patiño-Gómez, C. (2019). Dynamic modelling of the climate change impact in the Conchos River basin water management. *Tecnología y ciencias del agua*, 10(1), 207-233.

Minitab Inc. (2016). *Minitab 17 Statistical Software*. Computer Software. State College, USA: Minitab, Inc. Recovered from www.minitab.com



Oliva, C. S. H., Gaytán, J. R. C., & González, F. M. C. (2017). Estimación de datos faltantes de precipitación por el método de regresión lineal: caso de estudio Cuenca Guadalupe, Baja California, México. *Investigación y Ciencia de la Universidad Autónoma de Aguascalientes*, (71), 34-44.

Ordoñez-Gálvez, J. J. (2011). *Cartilla técnica: aguas subterráneas-acuíferos*. Lima, Perú: Global Water Partnership, South América. Sociedad Geográfica de Lima.

Paulhus, J. L., & Kohler, M. A. (1952). Interpolation of missing precipitation records. *Monthly Weather Review*, 80(8), 129-133.

Peña-Díaz, S. (2019). Condiciones hídricas en la Cuenca del Valle de México/Water conditions in the Valley of Mexico Basin. *Tecnología y ciencias del agua*, 10(2), 98-127.

Sánchez-Martínez, M., & Carvacho-Bart, L. (2011). Comparación de ecuaciones empíricas para el cálculo de la evapotranspiración de referencia en la Región del Libertador General Bernardo O'Higgins, Chile. *Revista de Geografía Norte Grande*, (50), 171-186.

Scanlon, B. R., Healy, R. W., & Cook, P. G. (2002). Choosing appropriate techniques for quantifying groundwater recharge. *Hydrogeology Journal*, 10(1), 18-39.

Steinitz, C., Faris, R., Vargas-Moreno, J. C., Huang, G., Lu, S. Y., Arizpe, O., & Baird, K. (2005). *Alternative futures for the region of Loreto. Mexico: Baja California Sur*. Cambridge, USA: Harvard University.



Vanderplank, S., Favoretto, F., Mascareñas, I., & Aburto, O. (2020). *San Basilio: biodiversidad y conservación*. San Diego, USA: International Community Foundation.

Velázquez-Zapata, J. A., & Troin, M. (2020). Uncertainty in the evaluation of climate change impacts over two Mexican Catchments. *Tecnología y ciencias del agua*, 11(1), 1-36.

Water UN. (2012). *Managing water under uncertainty and risk. The United Nations world water development report 4, UN Water Reports*. Paris, France: World Water Assessment Programme.

Wurl, J., Rodríguez, L. M., Cassassuce, F., Gutiérrez, G. M., & Velázquez, E. R. (2013). Geothermal water in the San Juan Bautista Londó aquifer, BCS, Mexico. *Procedia Earth and Planetary Science*, 7, 900-903.

WWAP, Programa Mundial de Evaluación de los Recursos Hídricos de la UNESCO. (2019). *Informe Mundial de las Naciones Unidas sobre el Desarrollo de los Recursos Hídricos 2019: No dejar a nadie atrás*. París, Francia: Organización de las Naciones Unidas para la Educación, la Ciencia y la Cultura.

Zhao, K. Y., Jiang, X. W., Wang, X. S., & Wan, L. (2021). Restriction of groundwater recharge and evapotranspiration due to a fluctuating water table: A study in the Ordos Plateau, China. *Hydrogeology Journal*, 29(2), 567-577.

